Anal. Chem. **2009,** *81,* 1969–1975

Direct Determination of the Enantiomeric Purity or Enantiomeric Composition of Methylpropionates Using a Single Capacitive Microsensor

Petra Kurzawski,[†] Anja Bogdanski,[‡] Volker Schurig,[‡] Reinhard Wimmer,[§] and Andreas Hierlemann*[,†]

Department of Biosystems Science and Engineering, ETH Zürich, CH-4058 Basel, Switzerland, Institute of Organic Chemistry, University of Tübingen D-72076, Tübingen, Germany, and Department of Biotechnology, Chemistry and Environmental Engineering, Aalborg University, DK-9000, Aalborg, Denmark

Capacitive enantioselective sensors have been demonstrated to provide antipodal signals upon dosage of, e.g., the enantiomers of methyl lactate or methyl-2-chloropropionate. In a next step, these sensors have been used to not only qualitatively determine the nature of the respective enantiomer or to quantitatively measure its concentration upon dosage in the pure form but to also assess the enantiomeric composition of mixtures by using only a single capacitive-type sensor. The enantioselective coating material consisted of a modified γ-cyclodextrin. It was shown that the absorption and desorption kinetics of the two enantiomers of, e.g., the methyl-2-chloropropionate, are sufficiently different and produce sensor signal features that enable an accurate determination of the enantiomeric purity and composition of the chiral analyte or mixture under investigation. The method even allows for detecting small impurities in commercially available samples labeled as 99% enantiomerically pure. Moreover, the results disclosed here show that sensor techniques can be used to reveal details of enantioselective analyte−receptor and analyte−matrix interactions.

Since the biological activity of many compounds depends on their chirality, it is of great importance to not only know which compound enantiomer is present but to also precisely determine the respective enantiomeric purity or enantiomeric composition.[1−6]

Chiral separation and sensor methods in gas and liquid phase predominantly rely on the usage of matrices that contain enantioselective receptor structures,[7−22] such as cyclodextrins,[7,8,11,17−19,21,23−34] or molecularly imprinted polymers.[15,16,20,35,36] The chiral recognition is, in most cases, based on the formation of a more stable diastereomeric complex with one of the enantiomers. A large Gibb's energy difference between the respective diastereomeric complexes entails a high enantioselectivity.

Signals of sensors functionalized with chiral recognition structures vary in their response magnitude[8,23,37−39] or, as discovered recently, in their response sign to the different enantiomers.[40] In both cases, a sensor signal at sorption equilibrium is not unequivocally correlated to a certain composition of

* To whom correspondence should be addressed. Fax: +41 61 387 3992. E-mail: andreas.hierlemann@bsse.ethz.ch.

[†] ETH Zürich.

[‡] University of Tübingen.

[§] Aalborg University.

(1) Stinson, S. C. *Chem. Eng. News* **2000**, *78*, 55 ff.
(2) Stinson, S. C. *Chem. Eng. News* **2001**, *79*, 79 ff.
(3) Stinson, S. C. *Chem. Eng. News* **2001**, *79*, 45 ff.
(4) de Camp, W. H. *Chirality* **1989**, *1*, 2–6.
(5) Izake, E. L. *J. Pharm. Sci.* **2007**, *96*, 1659–1676.
(6) Mei, X. F.; Wolf, C. *J. Am. Chem. Soc.* **2006**, *128*, 13326–13327.
(7) Schurig, V. *J. Chromatogr., A* **2002**, *965*, 315–356.
(8) Shahgaldian, P.; Pieles, U. *Sensors* **2006**, *6*, 593–615.
(9) Ward, T. J.; Hamburg, D. M. *Anal. Chem.* **2004**, *76*, 4635–4644.
(10) Diamond, D.; Nolan, K. *Anal. Chem.* **2001**, *73*, 22A–29A.
(11) Szejtli, J. *Chem. Rev.* **1998**, *98*, 1743–1753.
(12) Belder, D.; Ludwig, M. *Electrophoresis* **2003**, *24*, 2422–2430.
(13) Schreier, P.; Bernreuther, A.; Huffer, M. *Analysis of Chiral Organic Molecules*; Walter de Gruyter & Co., Berlin, New York, 1995.
(14) Subramanian, G., Ed. *A Practical Approach to Chiral Separations by Liquid Chromatography*; Verlag Chemie, VCH: Weinheim, Germany, 1994.
(15) Gübitz, G.; Schmid, M. G. *Mol. Biotechnol.* **2006**, *32*, 159–179.
(16) Hillberg, A. L.; Brain, K. R.; Allender, C. J. *Adv. Drug Delivery Rev.* **2005**, *57*, 1875–1889.
(17) Kieser, B.; Fietzek, C.; Schmidt, R.; Belge, G.; Weimar, U.; Schurig, V.; Gauglitz, G. *Anal. Chem.* **2002**, *74*, 3005–3012.
(18) Köhler, J. E. H.; Hohla, M.; Richters, M.; König, W. A. *Angew. Chem.* **1992**, *31*, 319–320.
(19) König, W. A.; Krebber, R.; Mischnick, P. *J. High Resolut. Chromatogr.* **1989**, *12*, 732–738.
(20) Li, W.; Li, S. J. In *Oligomers Polymer Composites Molecular Imprinting*, Springer, Berlin, Heidelberg, 2007; Vol. 206, pp 191−210.
(21) König, W. A.; Hochmuth, D. H. *J. Chromatogr. Sci.* **2004**, *42*, 423–439.
(22) Roussel, C.; Del Rio, A.; Pierrot-Sanders, J.; Piras, P.; Vanthuyne, N. *J. Chromatogr., A* **2004**, *1037*, 311–328.
(23) Bodenhöfer, K.; Hierlemann, A.; Juza, N.; Schurig, V.; Göpel, W. *Anal. Chem.* **1997**, *69*, 4017–4031.
(24) Szejtli, J. *Pure Appl. Chem.* **2004**, *76*, 1825–1845.
(25) Ozoemena, K. I.; Stefan, R. I. *Talanta* **2005**, *66*, 501–504.
(26) König, W. A. *Gas Chromatographic Enantiomer Separation with Modified Cyclodextrins*; Hüthig Buch-Verlag: Heidelberg, Germany, 1992.
(27) Easton, C. J.; Lincoln, S. F. *Chem. Soc. Rev.* **1996**, *25*, 163 ff.
(28) May, L. P.; Byfield, M. P.; Lindstrom, M.; Wunsche, L. F. *Chirality* **1997**, *9*, 225–232.
(29) Bodenhöfer, K.; Hierlemann, A.; Göpel, W.; Juza, M.; Gross, B.; Schurig, V. *Chim. Oggi* **1998**, *16*, 56–58.
(30) König, W. A. *Chirality* **1998**, *10*, 499–504.
(31) Fietzek, C.; Hermle, T.; Rosenstiel, W.; Schurig, V. *Fresenius' J. Anal. Chem.* **2001**, *371*, 58–63.
(32) Juvancz, Z.; Szejtli, J. *TrAC, Trends Anal. Chem.* **2002**, *21*, 379–388.
(33) Schmitt, U.; Branch, S. K.; Holzgrabe, U. *J. Sep. Sci.* **2002**, *25*, 959–974.
(34) Shahgaldian, P.; Hegner, M.; Pieles, U. *J. Inclusion Phenom. Macrocyclic Chem.* **2005**, *53*, 35–39.
(35) Mahony, J. O.; Nolan, K.; Smyth, M. R.; Mizaikoff, B. *Anal. Chim. Acta* **2005**, *534*, 31–39.
(36) Liu, F.; Liu, X.; Ng, S. C.; Chan, H. S. O. *Sens. Actuators, B* **2006**, *113*, 234–240.
(37) Trojanowicz, M.; Wcislo, M. *Anal. Lett.* **2005**, *38*, 523–547.
(38) Yin, X. L.; Ding, J. J.; Zhang, S.; Kong, J. L. *Biosens. Bioelectron.* **2006**, *21*, 2184–2187.
(39) Aboul-Enein, H. Y.; Stefan, R. I. *Crit. Rev. Anal. Chem.* **1998**, *28*, 259–266.

10.1021/ac802455c CCC: $40.75
Published on Web 02/03/2009

an enantiomeric mixture. In the case that the two enantiomers evoke different sensor response magnitudes it is impossible to determine the precise enantiomeric composition from the equilibrium signal as well as it is impossible in the case that the two enantiomers produce antipode signal signs, since there are always several possible mixture compositions and enantiomer concentrations that inevitably produce the same equilibrium signal values. Here we demonstrate that the kinetic signatures (evolution of a sensor signal with time) of a single capacitive chiral sensor that features antipode signals can be used to quantify the enantiomeric compositions of chiral compounds. The main reason is that the sorption kinetics and the respective analyte/receptor interaction mechanism of one of the enantiomers significantly differs from that of the corresponding other enantiomer. In this context it has to be mentioned that the technique described here is only applicable to pure samples of the respective analytes. In the presence of other analytes or impurities a single sensor is not sufficient, and an array of sensors featuring different selectivities has to be used.

The capacitive transducer used in this study is part of a multitransducer system[41,42] and features two sets of interdigitated electrodes that correspond to two capacitor plates.[43] The capacitor includes 128 finger pairs, electrode width and spacing are 1.6 μm, the measurement frequency is 600 kHz. The sensor monitors changes in the dielectric coefficient of the polymer upon analyte absorption. The capacitance changes upon analyte absorption are in the attofarad range and cannot be measured conventionally. Therefore, a differential measurement scheme has been applied that produces a frequency signal output, which is proportional to the occurring capacitance changes.[43−47] Details of the capacitance−frequency conversion are given in the Experimental Section.

Thick polymer layers (thicker than half the periodicity of the electrodes, for a detailed discussion see ref 48) have been used for the kinetic investigations, since the capacitive sensor response is then determined by three contributions, the dielectric coefficients of: (i) absorbed analyte, (ii) receptor matrix,[48,49] and (iii) that of the respective diastereomeric complexes.[40]

The sensitive layer consisted of chiral octakis(3-*O*-butanoyl-2,6-di-*O*-pentyl)-γ-cyclodextrin (Lipodex E)[19] dissolved (50% weight fraction) in a poly(dimethylsiloxane) matrix.[7,8,23] A second sensor chip coated with pure, achiral poly(dimethylsiloxane), PDMS, was used as a reference to monitor the dosed concentrations. For details, see the Experimental Section.

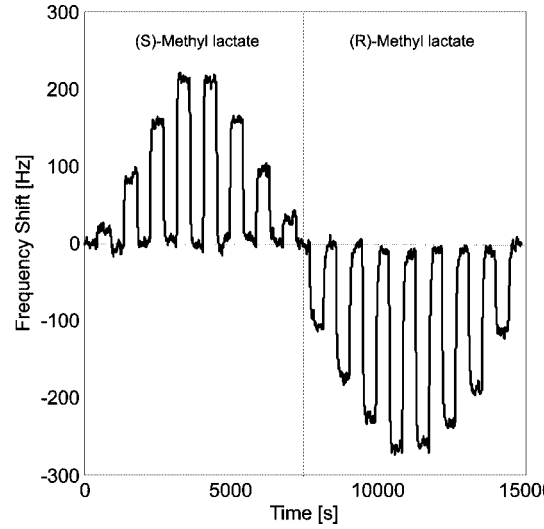

Figure 1. Measurement signals of the capacitive sensor upon exposure to the enantiomers of methyl lactate at concentrations of 10−40 ppm. The measurement data are given as frequency shifts due to the differential readout and digitalization (ref 47). For the devices used here 1 Hz corresponds to a capacitance change of 5.25 aF.

As has been reported in ref 40 and as shown in Figure 1 for methyl lactate (methyl-2-hydroxypropionate), and Figure 2a for methyl-2-chloropropionate, capacitive sensors provide antipodal signals upon dosage of the two enantiomers of these analytes at low concentrations (e.g., 10−40 ppm lactate, 20−80 ppm chloropropionate).

The negative signals upon dosage of the (*R*)-enantiomer of methyl lactate or the (*S*)-enantiomer of methyl-2-chloropropionate occur despite the fact that methyl lactate and methyl-2-chloropropionate exhibit dielectric coefficients of 31 and 15, respectively, which is considerably higher than that of the cyclodextrin/PDMS mixture (ε = 3.1). This behavior has been explained with molecular orientation effects as a consequence of the stronger interaction of the methyl lactate (*R*)-enantiomer and the chloropropionate (*S*)-enantiomer with the modified cyclodextrin.[40] These orientation effects have been assumed to produce a local compensation of partial charges in the receptor/enantiomer complex that entails a capacitance decrease. As is evident from Figures 1−4 and consistent with literature results the (*R*)-enantiomer of methyl lactate interacts more intensely with the modified γ-cyclodextrin than the (*S*)-enantiomer, and the (*S*)-enantiomer of methyl-2-chloropropionate interacts more intensely than the (*R*)-enantiomer.[7,23,50] Similar results have been obtained using a modified β-cyclodextrin (not shown), where, again in agreement with GC data from literature,[7,50] the (*S*)-enantiomer of methyl-2-chloropropionate interacted more intensely with the cyclodextrin than the (*R*)-enantiomer.

The sensor-signal-versus-analyte-concentration curves as displayed in Figure 2[40] are almost linear for the less intensely interacting enantiomer ((*R*)-methyl-2-chloropropionate, (*S*)-methyl lactate), which is characteristic for nonspecific physisorption processes (Henry-type sorption[23]). In the case of the preferentially sorbed enantiomer ((*S*)-methyl-2-chloropropionate, (*R*)-methyl

(40) Kurzawski, P.; Bogdanski, A.; Schurig, V.; Wimmer, R.; Hierlemann, A. *Angew. Chem., Int. Ed.* **2008**, *47*, 913–916.
(41) Hagleitner, C.; Hierlemann, A.; Lange, D.; Kummer, A.; Kerness, N.; Brand, O.; Baltes, H. *Nature* **2001**, *414*, 293–296.
(42) Kurzawski, P.; Hagleitner, C.; Hierlemann, A. *Anal. Chem.* **2006**, *78*, 6910–6920.
(43) Kummer, A. M.; Hierlemann, A.; Baltes, H. *Anal. Chem.* **2004**, *76*, 2470–2477.
(44) Hagleitner, C.; Hierlemann, A.; Baltes, H. In *Sensors Update*; Baltes, H., Fedder, G. K., Korvink, J. G., Eds.; Wiley VCH: Weinheim, Germany, 2003; Vol. 12, pp 51−120.
(45) Kummer, A.; Hierlemann, A. *IEEE Sens. J.* **2006**, *6*, 3–10.
(46) Hagleitner, C.; Hierlemann, A.; Brand, O.; Baltes, H. In *Sensors Update*; Baltes, H., Fedder, G. K., Korvink, J. G., Eds.; Wiley VCH: Weinheim, Germany, 2002; Vol. 11, pp 101−155.
(47) Hagleitner, C.; Lange, D.; Hierlemann, A.; Brand, O.; Baltes, H. *IEEE J. Solid-State Circuits* **2002**, *37*, 1867–1878.
(48) Kummer, A. Ph.D. Thesis, ETH Zurich, Zurich, Switzerland, 2004.
(49) Steiner, F. P.; Hierlemann, A.; Cornila, C.; Noetzel, G.; Bachtold, M.; Korvink, J. G.; Göpel, W.; Baltes, H. Proceedings of the 8th International Conference on Solid State Sensors and Actuators, Stockholm, Sweden, 1995; pp 814−817.
(50) Schurig, V. *TrAC, Trends Anal. Chem.* **2002**, *21*, 647–661.

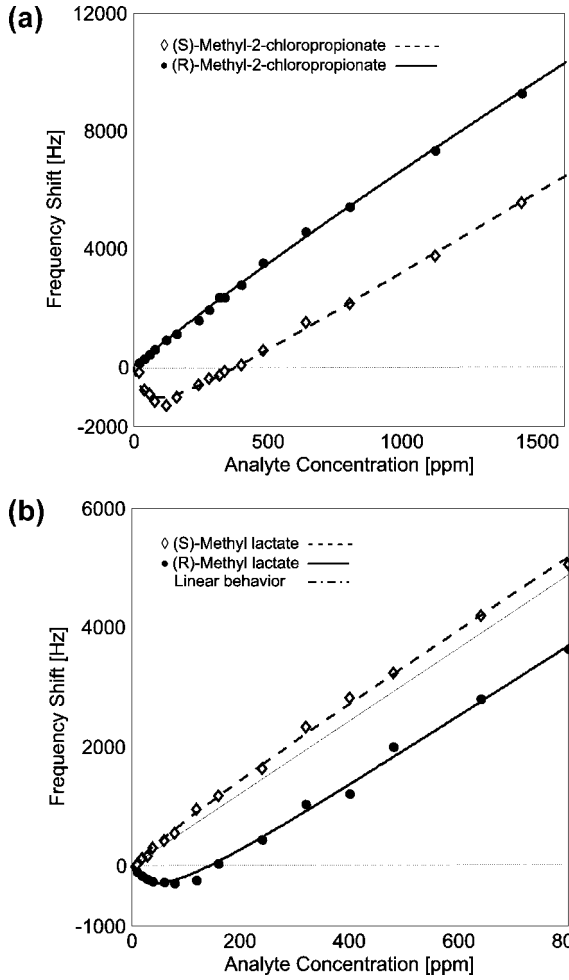

Figure 2. Capacitive sensor signals vs concentration upon dosage of (a) (*S*)- and (*R*)-methyl-2-chloropropionate and (b) (*S*)- and (*R*)-methyl lactate (ref 40). The lines serve as guides to the eye.

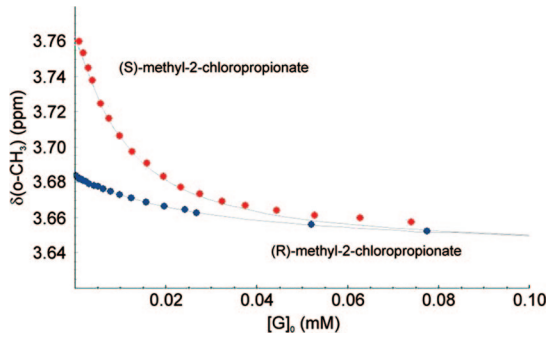

Figure 3. Chemical shift of the *O*-Me group of (*R*)- and (*S*)-methyl-2-chloropropionate vs their concentration in the presence of 3.6 mM octakis(3-*O*-butanoyl-2,6-di-*O*-pentyl)-γ-cyclodextrin in cyclohexane-d_{12}. The data points are depicted as solid dots; the lines represent the fits.

lactate), they feature a strongly curved low-concentration part going through negative territory, followed by a linear high-concentration part.[40] The low-concentration part can be best described as Langmuirian-type due to the limited number of sorption sites inside the cyclodextrin cages, whereas the high-concentration part is also of Henry-type.[23]

The shape of the sensor-signal-versus-analyte-concentration curves of the preferentially sorbed enantiomer ((*S*)-methyl-2-chloropropionate, (*R*)-methyl lactate) has been explained by the

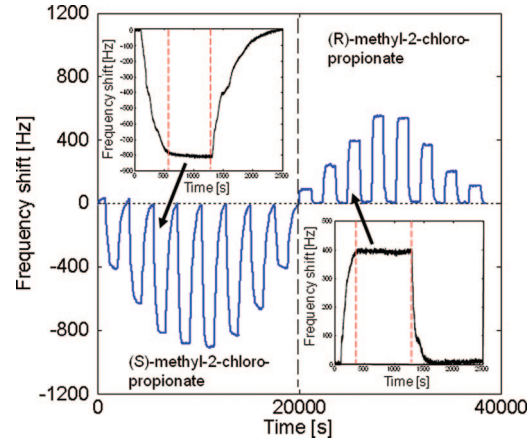

Figure 4. Measurement signals of the capacitive sensor upon exposure to the enantiomers of methyl-2-chloropropionate at different concentrations. The measurement data are given as frequency shifts due to the differential readout and digitalization (ref 47). For the devices used here 1 Hz corresponds to a capacitance change of 5.25 aF. Analyte concentrations: 20, 40, 60, 80 ppm; the close-ups show the kinetic sensor response signature for a step exposure of 60 ppm; the differences in the absorption and desorption characteristics of the two enantiomers are evident.

fact that the number of preferentially sorbed analyte molecules supersedes that of the cyclodextrin receptor molecules (1:1 complexation at approximately 100 ppm, Figure 2) upon increasing analyte concentration. The signal contribution of the orientation effect (dielectric coefficient decrease) is, therefore, more and more counterbalanced by the dielectric coefficient increase originating from analyte molecules, for which no more cyclodextrin cavities are available so that they nonspecifically absorb somewhere in the cyclodextrin/polymer matrix (Figure 2).[40] Finally at large concentrations, a capacitance increase is observed, which, however, is lower than that produced by the same concentration of the less intensely interacting enantiomer. This is due to the fact that the preferentially sorbed analyte molecules is still trapped within the cyclodextrin cavities so that a certain number of nonspecifically absorbed molecules is needed to counterbalance the capacitance-lowering effect of the trapped ones. The less intensely interacting enantiomers do not enter into close enough contact with the cyclodextrin torus to produce the above-mentioned orientation effects (Figures 1, 2, and 4).[40]

It has to be noted that the capacitive sensor signals reported on here represent a convolution of (i) the analyte sorption thermodynamics as also observed by GC or mass-sensitive sensors[23] and (ii) transducer-specific analyte-induced effects on the dielectric properties of the overall layer (molecular orientation effects). A direct comparison of sensor data with chiral discrimination factors, α, commonly employed in GC (methyl-2-chloropropionate, 4.19; methyl-2-lactate, 1.54 at 303 °K), is not possible due to the occurrence of negative and positive sensor signal signs.

Nuclear Overhauser effect spectroscopy (NOESY) measurements have been conducted for methyl-2-chloropropionate and evidenced a mechanistic difference in the interaction of the two enantiomers with the cyclodextrin receptor suggesting that the (*S*)-enantiomer of methyl-2-chloropropionate penetrates deeper into the cavity in comparison to the (*R*)-enantiomer.[40] This is also reflected in the chemical shifts and the NMR-derived association constants that have been determined from fits to the data points

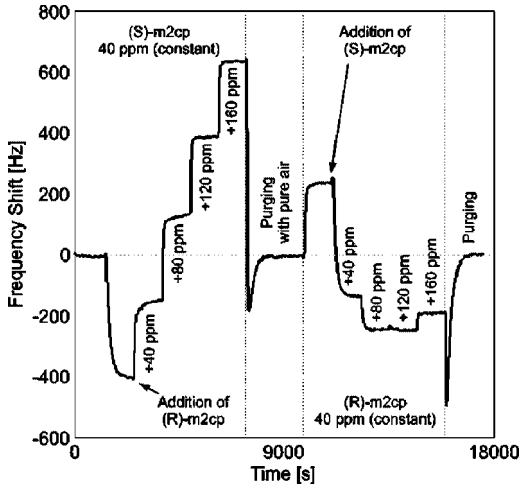

Figure 5. Measurement signals of the γ-cyclodextrin-coated capacitive sensor upon dosage of mixtures of different methyl-2-chloropropionate (m2cp) enantiomeric composition. For the sorption−equilibrium signal assessment the sensor was constantly exposed to the analytes. First 40 ppm of one of the enantiomers was dosed to the sensor, then the concentration of the other enantiomer was stepwise increased in four steps of 40 ppm. Note that the sorption equilibrium response values of both racemates (second exposure step of each series: 40 ppm (*R*) plus 40 ppm (*S*)) are expectedly identical.

of an NMR titration. The chemical shifts of the methoxy groups upon association with the cyclodextrin torus are significantly different for both enantiomers (Figure 3). The association constants amount to 193 ± 20 M^{-1} for (*S*)- and 45 ± 5 M^{-1} for (*R*)-methyl-2-chloropropionate. The determination procedure of the association constants based on the data displayed in Figure 3 is described in the Experimental Section.

EXPERIMENTAL SECTION

Relation of Frequency Shift to Capacitance Change. The capacitance change upon analyte absorption within a polymer is in the attofarad range. A second-order sigma-delta-modulator (ΣΔ-modulator) differential measurement with the polymer-coated sensing capacitor, C_S, and a passivated reference, C_{ref}, has been used to assess such minute capacitance changes.[47,51] With the preset reference and feedback capacitances a change in the output signal, Δf_{out}, can be directly assigned to a change in the sensor capacitance, ΔC_S, via

$$\Delta C_S = \frac{2C_{fb}}{f_{clk}}\Delta f_{out} \approx 5.25\frac{aF}{Hz}\Delta f_{out} \quad (1)$$

For an uncoated sensing capacitor the absolute value of the interdigitated capacitors (C_S and C_{ref}) is approximately 8 pF.[51] To estimate the additional capacitance of the polymer layer the output frequency of a capacitor was measured before and after applying the polymer layer of γ-cyclodextrin/PDMS (50% (w/w)). A frequency shift of Δf_{out} = 151.5 kHz was determined, which corresponds according to eq 1 to a capacitance of only 0.8 pF. The total capacitance of the polymer layer amounts to $C_{coating}$ = 1.68 pF after relating the capacitance of the coated device to that of an "air-filled" uncoated sensor. Since the dielectric constants of the different cyclodextrin/PDMS layers are very similar to that of the polymer PDMS alone (γ-cyclodextrin ε = 4.1; PDMS ε = 2.8) their capacitance contributions should be in the same range.

Sensitive Layers and Deposition. After completion of the CMOS process and after packaging, the polymer films that act as chemically sensitive layers have been deposited onto the sensor structures by means of spray-coating using an airbrush (Badger, model 200-F, Franklin Park, IL). The airbrush has been fixed at a distance of 10 cm from the chip. A specially designed silicon shadow mask that also could be precisely aligned on the packaged chip has been used to cover the circuitry as well as the capacitive reference sensors. Only the sensing elements of the system were exposed to the spray-coating. Octakis(3-*O*-butanoyl-2,6-di-*O*-pentyl)-γ-cyclodextrin[19] has been mixed with PDMS (Silicone GE SE-30, Supelco, Bellefonte, PA), at 50% (w/w) using dichloromethane as a solvent and then deposited on the transducers. Reference chips to monitor the dosed concentrations have been coated with pure, achiral PDMS. After the layer deposition the polymer coatings were cured in a saturated dichloromethane atmosphere for 2 min, so that smooth layers on the sensing elements were obtained.

Gas Manifold. For gas tests, the CMOS chips were mounted on dual in-line packages and then loaded into the measurement chamber of a computer-controlled gas manifold. Measuring fast sensor signal transients requires a careful design of the gas manifold so that the signal dynamics reflect the analyte sorption and desorption kinetics rather than the gas flow dynamics of the setup. Thus, all gas switching processes must be fast in comparison to the analyte sorption dynamics. To this end, a manifold and flow setup was used, the most important features of which include a cross-over flow architecture by use of a fast four-way valve, matched flow resistances of the two output gas lines of the four-way valve, and a small tubing volume between the valve and the sensor measurement chamber. This setup, details of which have been described in ref 52, can provide sharp analyte concentration steps.

The analyte vapors were generated from specifically developed temperature-controlled (T = 223−293 K) vaporizers[53] using synthetic air as a carrier gas and then diluted as desired using computer-driven mass-flow controllers. The vapor-phase concentrations at the respective temperatures were calculated following the Antoine equation.[54] A photoacoustic detector (infrared light for excitation, 1314 photoacoustic multigas monitor, Innova Airtec Systems, Denmark) has been used as an independent reference to assess the actual analyte gas-phase concentrations.

Sensors featuring enantioselective and achiral coatings have been simultaneously measured in a temperature-regulated flow-through chamber (303 K) at a sampling frequency of 1.5 Hz.[52] Both gas streams (pure carrier gas and carrier gas with analyte) were thermostabilized to the measurement chamber temperature before entering the chamber itself. Typical experiments consisted of alternating exposures to pure air and analyte-loaded air (20 min exposure intervals to reach steady state or thermodynamic sorption equilibrium states).

(51) Hagleitner, C. Ph.D. Thesis, ETH Zurich, Zurich, Switzerland, 2002.

(52) Kummer, A. M.; Burg, T. P.; Hierlemann, A. *Anal. Chem.* **2006**, *78*, 279–290.

(53) Bodenhöfer, K.; Hierlemann, A.; Schlunk, R.; Göpel, W. *Sens. Actuators, B* **1997**, *45*, 259–264.

(54) Riddick, J. A.; Bunger, W. B.; Sakano, T. K. *Organic Solvents*, 4th ed.; Wiley Interscience: New York, 1986.

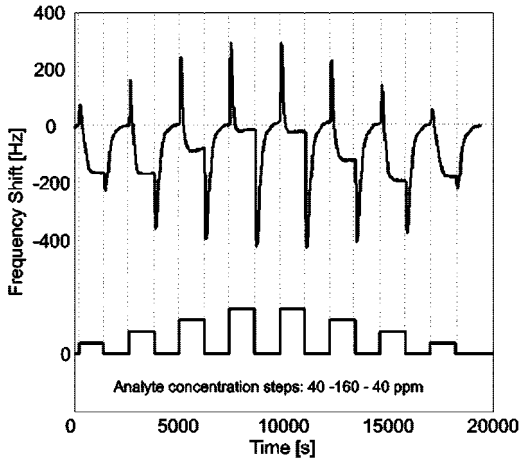

Figure 6. Interval dosage signal characteristics of the capacitive sensor upon exposure to racemic mixtures of methyl-2-chloropropionate at total concentrations of 40, 80, 120, and 160 ppm.

Analytes. The selected analytes included, on the one hand, standard organic solvents that were used as purchased from Fluka, Buchs, Switzerland without further purification (*n*-octane, toluene, methyl propionate, etc.). On the other hand it included chiral analytes, i.e., both enantiomers of methyl lactate (enantiomeric purity 98%, Sigma-Aldrich AG, Steinheim, Germany), and both enantiomers of methyl 2-chloropropionate (enantiomeric purity >99%, Sigma-Aldrich AG, Steinheim, Germany) as well as racemic mixtures (Sigma-Aldrich AG, Steinheim, Germany) that have been dosed to the sensors without further purification.

Determination of NMR Association Constants. A sample of 4 mM octakis(3-*O*-butanoyl-2,6-di-*O*-pentyl)-γ-cyclodextrin in cyclohexane-d_{12} was titrated with small aliquots of a solution of 1 M methyl-2-chloropropionate. The chemical shifts of the methyl-2-chloropropionate resonances (δ_{obs}) were plotted against the total concentration of methyl-2-chloropropionate ($[G]_0$).

$$\delta_{obs} = \frac{[HG]}{[G]_0}\delta_{bound} + \frac{[G]_0 - [HG]}{[G]_0}\delta_{free} \quad (2)$$

$$[HG] = 0.5([H]_0 + [G]_0 + (1/K)) \pm \sqrt{([H]_0 + [G]_0 + (1/K))^2 - 4[H]_0[G]_0} \quad (3)$$

where δ_{bound} is the chemical shift between free and bound methyl-2-chloropropionate, [HG] is the concentration of the associated complex, $[G]_0$ is the total concentration of methyl-2-chloropropionate, $[H]_0$ is the total concentration of octakis(3-*O*-butanoyl-2,6-di-*O*-pentyl)-γ-cyclodextrin, and K_a is the association constant of the complex formation. Only one of the two solutions yields physically meaningful results. K_a and δ_{bound} were determined by fitting eqs 2 and 3 to the experimental data with the nonlinear regression module of Mathematica 3.0.

RESULTS AND DISCUSSION

Here we want to first have a closer look at the characteristic features in the temporal signal evolution during dosage of the pure enantiomers of methyl-2-chloropropionate (Figure 4) and during dosage of mixtures of different enantiomeric compositions (Figures 5−7). The sensitive layers for these measurements were approximately 4 μm thick so that the region of the electrical field was completely filled with sensitive matrix.[43]

Table 1. t_{90} Times (t_{90}, Rise Time, at Which Signal Reaches 90% of the Equilibrium Value) and t_{10} Times (t_{10}, Decay Time upon Dosage End, at Which the Signal is Down to 10% of the Equilibrium Value) in Seconds for Both Enantiomers, (*R*)- and (*S*)-Methyl-2-chloropropionate, Averaged Over Different Measurements[a]

	rise time t_{90}				fall time t_{10}			
concentration [ppm]	(*R*): t_{90} [s]	SD [s]	(*S*): t_{90} [s]	SD [s]	(*R*): t_{10} [s]	SD [s]	(*S*): t_{10} [s]	SD [s]
20	226	6	700	54	260	27	670	9
40	190	11	370	10	240	24	660	13
60	174	2	320	10	220	31	660	14
80	160	2	270	10	210	29	620	5

[a] The times are given in seconds and denote the interval between the time of switching the valve and the time of passing the respective thresholds (90% or 10% of the equilibrium signal value). The gas-manifold dead time between switching the valve and the analyte reaching the sensors is less than 1 s.

Figures 1 and 4 show antipodal signals upon interval dosage of the two pure enantiomers of methyl lactate and methyl-2-chloropropionate at concentrations below full receptor coverage or full cyclodextrin occupation, which occurs at approximately 100 ppm. The signals are either only negative or only positive and do not show any features at the dosing onset or stop. There are, however, differences in the response kinetics. The responses to the (*S*)-enantiomer, which forms the stronger associated complex with the cyclodextrin, show a slower response decrease as can be seen in the insets in Figure 4. These insets show one single exposure step (60 ppm) at high temporal resolution. The occurrence of receptor/analyte molecular orientation effects also seems to delay the time at which an equilibrium or steady-state signal is reached (see insets in Figure 4).

A more detailed statistical analysis of the signal rise and decay times is displayed in Table 1 and reveals a large difference in the t_{90} times and t_{10} times for the two enantiomers. Both t_{90} times and t_{10} times are significantly longer for the (*S*)-enantiomer and show a more pronounced concentration dependence for the t_{90} times as compared to the t_{10} times. Similar concentration dependence, i.e., a faster reaching of the sorption equilibrium for higher concentrations, has also been observed for polymers like poly(epichlorohydrin) in previous studies: concentration-dependent diffusion constants usually exponentially increase with the analyte concentration.[52] The difference in response or sorption kinetics between the two enantiomers can be used for a quantitative analysis of enantiomer mixtures with a single sensor as will be shown now.

First, experiments without purging intervals between the different concentration- or enantiomeric-composition steps were conducted to assess the characteristics of the steady-state signals. The sensor responses upon dosing one enantiomer (40 ppm) and gradually adding more and more of the other enantiomer (40−160 ppm) are shown in Figure 5.

The respective equilibrium values do not directly provide quantitative information, since it is impossible to unequivocally correlate a certain sensor signal to a precise enantiomeric composition. This holds particularly true for adding higher (*S*)-enantiomer concentrations to 40 ppm (*R*)-enantiomer, where the signal does not change much as a consequence of a complete occupation of the cyclodextrin

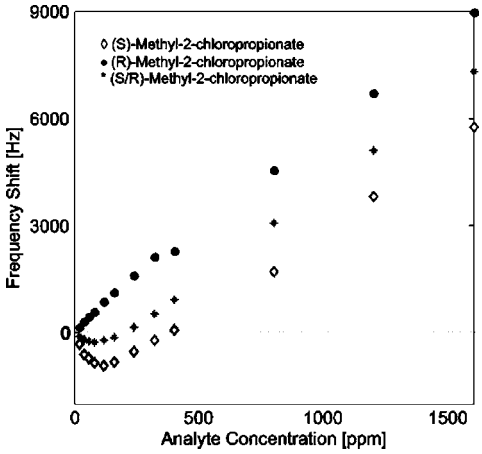

Figure 7. Comparison of the measurements of the pure enantiomers of methyl-2-chloropropionate and the racemic mixture of the capacitive sensor.

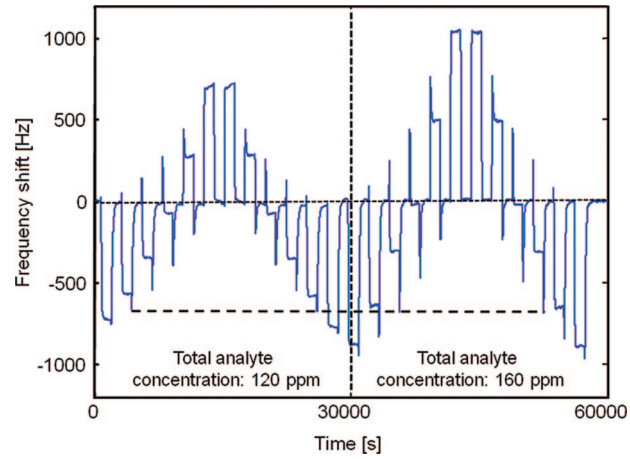

Figure 8. Measurement signals of the γ-cyclodextrin-coated capacitive sensor upon interval dosage of mixtures of different enantiomeric composition of methyl-2-chloropropionate. The overall analyte concentration was kept constant during each series (120 or 160 ppm); however, the fractions of both enantiomers varied in 20% steps. The sensor was exposed to pure (*S*)-enantiomer, then the fraction of the (*S*)-enantiomer was reduced and that of the (*R*)-enantiomer increased in 20% steps until dosage of the pure (*R*)-enantiomer. Afterward, the same steps were applied in reverse order.

receptors (Figure 5, right side: addition of 80−160 ppm of (*S*)-enantiomer). In Figure 5 there are also no features visible at the onset or beginning of a new concentration interval; however, there are two negative peaks at the end of the two dosage sequences before the signal returns to the baseline. These negative peaks can be assigned to the comparably slow release of the (*S*)-enantiomer, 40 ppm at the end of the left-hand sequence and 160 ppm at the end of the right-hand sequence.

In a next step, an interval dosing strategy was applied with purging time allotted between the different exposure steps. As is obvious from Figures 6 and 8, the responses upon interval dosage of enantiomeric mixtures show, in contrast to dosings of pure enantiomers at low concentrations (Figure 4), very distinct dynamic signal characteristics: there is strong initial upward signal peak, then the capacitance decreases and trends toward an equilibrium value. Upon switching off the analyte supply there is a strong overshoot in the negative direction, which can also be seen in Figure 5 at each dosing sequence end.

Figure 6 shows the signals upon dosing racemic mixtures of different overall concentrations (40, 80, 120, and 160 ppm) to the sensors. The system was always purged with pure synthetic air in between the exposure intervals. The amplitudes of the positive and negative peaks upon dosage onset and dosage stop are obviously correlated to the overall racemate concentration: they increase and decrease in dependence of the concentration. The exact time stamp of the peak is also slightly concentration-dependent, the positive peak occurs earlier for increasing concentrations, the negative somewhat later (shifts of 5−10 s). The steady-state or equilibrium signal is more negative for lower concentrations as can be expected, since the amplitude of the (*S*)-enantiomer negative signals in Figure 4 clearly exceeds that of the (*R*)-enantiomer positive signals, before, at larger concentrations, a signal saturation (full occupation of the cyclodextrin units) and reversal occurs.[40]

The evolution of equilibrium signal levels upon varying the concentration of a racemic mixture as compared to the equilibrium signals of the pure enantiomers is displayed in Figure 7. Upon exposure to the racemic mixture the capacitive sensors yield a signal that lies in between those of the two pure enantiomers. In having a more detailed look at the racemate signals it becomes evident that, at low concentrations, the signals more or less constitute a superposition of the signals of both enantiomers at half the concentration of the racemic mixture. This can be observed in Figure 5: the equilibrium signal of 40 ppm (*S*)-chloropropionate is −400 Hz, that of 40 ppm (*R*)-enantiomer is +250 Hz so that a linear superposition yields −150 Hz, whereas the arithmetic mean value would be approximately −80 Hz. The racemate composed of 40 ppm of each enantiomer is −150 Hz. At higher concentrations, there are mixing effects and a competitive process for sorption at the preferential and nonpreferential sites in the composite matrix.

Figure 8 shows the interval dosage signal characteristics of the capacitive sensor upon exposure to mixtures of different methyl-2-chloropropionate enantiomeric compositions at two different overall concentrations (120 ppm and 160 ppm). The overall analyte concentration was kept constant during each series, whereas the fractions of both enantiomers varied: First, the sensor was exposed to pure (*S*)-enantiomer at a concentration of 120 or 160 ppm, then the fraction of the (*S*)-enantiomer was reduced and that of the (*R*)-enantiomer was increased in 20% steps to finally arrive at the pure (*R*)-enantiomer. Afterward, the same steps were applied in reverse order. It is important to note that the same absolute (*S*)-enantiomer concentration produced identical signal amplitudes of the respective negative peaks in Figure 8: 96 ppm of the (*S*)-enantiomer evoked a signal of approximately −700 Hz, either in the 80% (*S*), 20% (*R*) mixture at 120 ppm total concentration, or in the 60% (*S*), 40% (*R*) mixture at 160 ppm total concentration. This is indicated by the dashed line.

The specific mixture signal characteristics confirm that, indeed, different interaction processes featuring distinct kinetics do occur for the two enantiomers. Since there is generally no positive dosage-onset peak for (*S*)-enantiomer exposures (see Figure 4 and signals in ref 40), it can be concluded that all (*S*)-molecules directly undergo the stronger host/guest complexation until a complete occupation of the cyclodextrin units is reached. The positive peaks in Figures 6 and 8 can, therefore, only be due to (*R*)-enantiomer molecules that nonspecifically interact with the

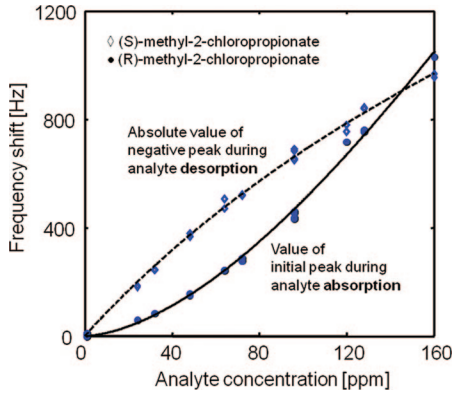

Figure 9. Capacitive sensor signal calibration obtained from mixtures of (*S*)- and (*R*)-methyl-2-chloropropionate as displayed in Figure 8: peak heights vs enantiomer concentrations. The plots are nonlinear, and absolute values instead of negative values are given for the (*S*)-enantiomer desorption peak. The dashed and the solid lines only serve as guides to the eye.

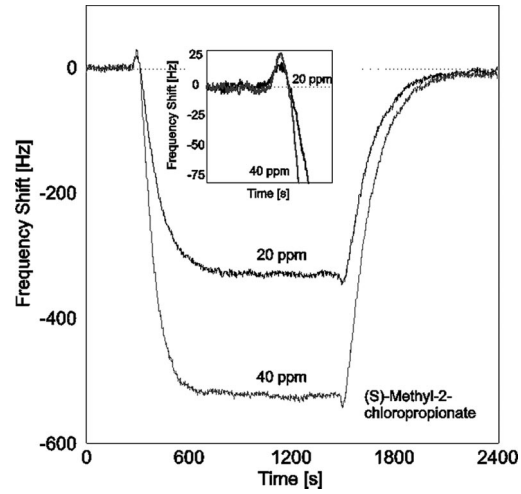

Figure 10. Sensor responses upon dosage of an industrial sample of a slightly impure (*S*)-methyl-2-chloropropionate (20 and 40 ppm total concentration), which contains 1.8% (*R*)-enantiomer as has been confirmed by enantioselective GC analysis using a commercially available Lipodex E column. The heights of the two peaks are depending on the total concentration.

receptor without experiencing molecular orientation effects and which show faster absorption and desorption characteristics. In turn, negative peaks only occur in the presence of the (*S*)-enantiomer as a consequence of its slower desorption kinetics (see also Figures 4 and 5).

Therefore, the positive analyte onset peak can be used to quantify the (*R*)-enantiomer and the negative peak upon purging can be used to quantify the (*S*)-enantiomer, since each of these features is evoked exclusively by one of the enantiomers. This quantification is possible over a rather wide range of concentrations: a calibration curve from several independent measurements is shown in Figure 9. Since the sensor signals upon different concentrations of the individual enantiomers (see ref 40) do not show linear characteristics, the calibration curves for the mixtures are also not expected to be linear. The calibration cannot be made by using pure analytes but has to be done with mixtures, since the two enantiomers most probably compete for the sorption sites inside the cyclodextrin torus, though only the (*S*)-enantiomer undergoes the previously described molecular orientation effects.[40]

After calibration a single sensor can, indeed, be used for the immediate and fast on-line detection of the enantiomeric composition and the total analyte concentration, since it simultaneously provides three values per exposure: (a) the analyte dosage-onset peak amplitude, (b) the dosage-stop peak amplitude, and (c) the steady-state or equilibrium level value. The exact time stamp of both peaks can potentially be used as additional input. Even enantiomeric impurities in practically relevant industrial samples at levels as low as 1.5−2% have been detected as shown in Figure 10.

Figure 10shows the capacitive sensor responses upon dosage of a commercial sample (labeled as 99% enantiomerically pure) of (*S*)-methyl-2-chloropropionate (20 and 40 ppm total concentration). Upon evaluation of the sensor signals it was decided that this sample cannot be used for our experiments and a subsequent enantioselective GC analysis confirmed that the sample contained in fact 1.8% (*R*)-enantiomer. The heights of the two peaks in Figure 10 are depending on the total concentration. Pure analytes with an impurity of less than 0.4%, tested and confirmed by GC measurements, do not show such peak features at low concentrations below complete cyclodextrin occupation as can also be seen in Figure 4.

In summary, it has been shown that a single capacitive sensor, which provides antipodal signals upon exposure to the enantiomers of 2-substituted methyl propionates, can also be used to rapidly determine the enantiomeric purity and composition of these important industrial chemicals on-line. The sensor method can detect impurities down to approximately 0.5−1%, which is, of course, inferior to a thorough GC analysis (less than 0.1%), so that a sensor could be used to prescreen chemicals, followed by a more detailed analysis for conspicuous samples. Moreover, simple capacitive sensors can be used to reveal detailed information on the kinetics of the involved sorption and partitioning processes. It is striking that the two enantiomers of the same compound show such large differences in their sorption kinetics, which, along with gas chromatographic (i.e., thermodynamic) and NMR spectroscopic evidence,[40] indicates that the occurring interaction processes are significantly different for both enantiomers with respect to thermodynamics and kinetics. Hence, the precision of the sensor measurements is assumed to be proportional to both, the thermodynamic and the kinetic enantioselectivity of the complexation process. For the system considered here a more stable diastereomeric complex forms more slowely than the less stable one so that the thermodynamic and kinetic enantioselectivities exhibit opposite signs. This probably is a common situation, rather than an exception with another example reported and discussed in ref 55. The findings reported on here can probably be extended to other chiral analytes.

ACKNOWLEDGMENT

Financial support for this work was provided within the framework of a European Network of Excellence, GOSPEL, FP6-IST-507610, by the Swiss Bundesamt für Bildung and Wissenschaft.

Received for review November 19, 2008. Accepted January 5, 2009.

AC802455C

(55) Kurganov, A. A.; Ponomareva, T. M.; Davankov, V. A. *Dokl. Akad. Nauk SSSR* **1987**, *293*, 623–626.